

## Anisotropic thermal conductivity of a fluid in a system of microscopic slit pores

S. Murad and P. Ravi

*Chemical Engineering Department, University of Illinois at Chicago, Chicago, Illinois 60680-4348*

J. G. Powles

*Physics Laboratory, University of Kent, Canterbury, Kent, CT2 7NR United Kingdom*

(Received 17 March 1993)

We report nonequilibrium-molecular-dynamics studies of a simple fluid in an infinite system of plane slit micropores, with walls of variable permeability. Our results show that the thermal conductivity of fluids in such constrained geometry can exhibit strong anisotropy, especially when the pore walls are almost impermeable. We show this in simulations of fluid systems for substances that are only anisotropic on an atomic, as opposed to a macroscopic, scale.

PACS number(s): 44.30.+v, 66.60.+a

### INTRODUCTION

Recently, we reported an alternative technique for studying fluids in constrained flow geometries, such as micropores [1,2]. The method permits the permeability of the wall to the enclosed fluid to be controlled precisely, while maintaining the atomic nature of the wall. We have already reported on the anisotropy of the self-diffusion coefficient as a function of the permeability of the walls (see Fig. 3 for a typical result). We have now used this alternative method, in conjunction with the nonequilibrium-molecular-dynamics technique (NEMD) [3–5], to examine the thermal conductivity of a Lennard-Jones fluid in a slit micropore. Our results clearly show that thermal conductivity in such systems is anisotropic. We are unaware of any previous simulations or experiments that have indicated such anisotropy of thermal conductivity in fluid systems, although anisotropy has been observed for diffusion coefficients in both simulation [1,6,7] and experiment [7,8].

### METHOD

Both the method for studying fluids in confined geometries and the nonequilibrium-molecular-dynamics technique have been described in detail in other recent publications [1–5], so we will only provide a brief summary here.

The simulation is based on the usual algorithm, in which all particles are initially at their fcc sites in the basic replicated cube of side  $L$ . To form the walls of the slit pore, all particles on one  $yz$  face of the cube are permanently tethered to their initial fcc sites by a tethering potential

$$\phi_T^*(d^*) = \frac{1}{2} K^* d^{*2}, \quad (1)$$

where  $d^* \equiv d/\sigma$  is the reduced scalar distance between the center of mass of a tethered particle and the tether site, and  $K^* \equiv K\sigma^2/\epsilon$ , where  $K$  is the force constant, which, as will be shown later, is an effective parameter for controlling the wall permeability.  $\epsilon$  and  $\sigma$  are the in-

teraction energy and distance parameters for the Lennard-Jones shifted-force (LJSF3) intermolecular potential, with a cutoff distance of 3.0. This potential acts between all particles, including those that are tethered. Such a scheme would, for example, in a 108-particle simulation, lead to 18 particles being tethered to form a slit pore wall. However, because of the periodic boundary conditions, this actually generates an infinite system of infinite parallel plane walls, with separation  $L$  [1]. Such a model leads to a realistic description of a slit pore system, as was found in our previous investigations using this model to study properties such as density profiles, diffusion coefficients, and wall permeabilities. The results obtained were found to reproduce all the main features of previous experimental and theoretical studies [1,2]. The diffusion of the atoms in many such systems has been studied in considerable detail [1,2]. For this transport property, thermal conductivity, we find it more convenient and more computationally effective to use the NEMD method rather than the correlation-time method which is conventional for homogeneous liquids [9] just as it was not suitable for the diffusion measurements.

The NEMD method creates an effective gradient in the system via an external field, and the resulting flux is measured to calculate the desired linear response. The equations of motion that need to be solved are [3,5]

$$\dot{\mathbf{r}}_i = \mathbf{p}_i / m, \quad (2)$$

$$\begin{aligned} \dot{\mathbf{p}}_i = & \sum_j \mathbf{f}_{ij} + (E_i - \bar{E}) \mathbf{F}(t) + \frac{1}{2} \sum_j \mathbf{f}_{ij} [\mathbf{r}_{ij} \cdot \mathbf{F}(t)] \\ & - \frac{1}{2N} \sum_{j,k} \mathbf{f}_{jk} [\mathbf{r}_{jk} \cdot \mathbf{F}(t)] - \alpha \mathbf{p}_i, \end{aligned} \quad (3)$$

where  $\mathbf{f}_{ij} = -\partial\phi_{ij}/\partial\mathbf{r}_i$ , and  $\phi_{ij}$  is the intermolecular interaction between all particles in the system.  $\mathbf{r}_i$  is the position vector of particle  $i$ ,  $\mathbf{p}_i$  is its momentum,  $E_i$  is its energy, and  $\bar{E}$  is the average energy per particle.  $\mathbf{r}_{ij} = \mathbf{r}_i - \mathbf{r}_j$  and  $N$  is the number of particles in the basic simulation cell.  $\mathbf{F}$  is the external field, which in our case is kept constant with time. Also, in our case  $\mathbf{F}$  had only

one nonzero Cartesian component at a time, that being along the direction in which we wished to calculate the thermal conductivity.  $\alpha$  is the usual thermostatting multiplier [3,5] to ensure constant total translational kinetic energy, i.e., to maintain the temperature constant in spite of the dissipative perturbation. It should be noted that this ingenious scheme [3,4] does not actually apply a temperature gradient. This would give at best a  $k$ -dependent thermal conductivity where  $k_{\min} = 2\pi/L$ ,  $L$  being typically  $20 \text{ \AA}$  in our simulation. It yields the  $k \rightarrow 0$ , i.e., the macroscopic thermal conductivity. The external field  $\mathbf{F}$ , plays the role of  $\text{grad} \ln T$ , in the zero-field limit [cf. Eq. (4)] in the usual Fourier heat-flow formula.

The thermal conductivity perpendicular to the pore wall could then be obtained from  $\lambda_{\perp}$ , which is  $\lambda_x$  in our case,

$$\lambda_{\perp} = \frac{1}{T} \frac{\langle J_x^Q(t \rightarrow \infty) \rangle}{F_x(t)}, \quad (4)$$

where  $T$  is the temperature. The heat-flux vector,  $\mathbf{J}^Q$  is given by

$$\mathbf{J}^Q = \frac{1}{V} \left[ \sum_i E_i \frac{\mathbf{p}_i}{m} + \frac{1}{2} \sum_{i,j} \mathbf{r}_{ij} \left[ \frac{\mathbf{p}_i}{m} \cdot \mathbf{f}_{ij} \right] \right], \quad (5)$$

where  $V = L^3$  is the volume of the simulation cube. We similarly calculate  $\lambda_{\parallel} = \lambda_y = \lambda_z$ , the thermal conductivity in directions parallel to the partially permeable walls.

The values of  $\lambda$  reported are thought to have an uncertainty of about  $\pm 10\%$ . The uncertainty can, of course, be reduced by performing longer runs. It should be noted that the thermal conductivity reported here is for the entire system, not just for the liquid, as this is the property of interest in such systems and the one most likely to be measured experimentally. One could also calculate the thermal conductivity of the fluid away from the pore wall (where the fluid molecules only interact with other fluid molecules). However, that would not really be the true thermal conductivity of the fluid inside the pore, since the fluid far from the pore walls behaves almost like a homogeneous fluid [2]. Near the wall, as can be seen from Eq. (5), the contributions from the fluid and the wall can only be separated on an *ad hoc* basis which we preferred not to do. On the other hand, the diffusion coefficient is for liquid only since the wall molecules do not diffuse but only vibrate.

## RESULTS AND DISCUSSION

All simulations had 108 particles in the basic cell, with  $\rho^* \equiv \rho\sigma^3 = 0.5$ ,  $T^* \equiv kT/\varepsilon = 1.0$ . Then,  $L^* \equiv L/\sigma = 6.0$ . The simulation consisted of 200 000 time steps of size  $\Delta t^* = 0.001$ , where  $t^* \equiv (\varepsilon/m\sigma^2)^{1/2}t$ , after 50 000 rejected equilibration steps. The usual tests to ensure non-dependence of the thermal conductivity values on the magnitude of the external field strength were also carried out. In fact,  $F^*$  varied from 0.05 to 0.10 in our simulations which satisfied this criterion.

For  $K^*$  small, e.g., for our lowest value 1, the tethered particles are almost as free to move as the "free" particles and then we expect that  $\lambda_{\perp} \approx \lambda_{\parallel} \approx \lambda_H$  where  $\lambda_H$  is the

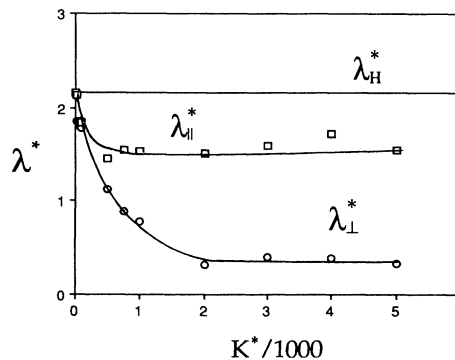


FIG. 1. Thermal conductivity  $\lambda$  of a Lennard-Jones (LJ SF 3) liquid confined in an infinite system of infinite plane atomic pores. The mean number density is  $0.5\sigma^{-3}$  and the temperature is  $1.0\varepsilon/k_B$ . The slit walls have a spacing of  $6\sigma$ . The spring constant of the tethered atoms of the wall is  $K^*\varepsilon/\sigma^2$ . For  $K^* \leq 10$  the walls are permeable to the liquid atoms and for  $K^* \geq 1000$  they are almost impermeable.  $\lambda = (k_B/\sigma^2)(\varepsilon/m)^{1/2}\lambda^*$ .  $\lambda_H$  is for the homogeneous "free" liquid ( $K=0$ ).  $\lambda_{\perp}$  is for heat flow perpendicular to the slit walls.  $\lambda_{\parallel}$  is for heat flow parallel to the slit walls. The error of measurement is about  $\pm 10\%$ . The points are joined by lines to guide the eye.

thermal conductivity of the corresponding homogeneous liquid. This is found to be so since we know that for this LJSF3 fluid in this state,  $\lambda_H^* \equiv (\sigma^2/k_B)(m/\varepsilon)^{1/2}\lambda_H = 2.1$ , as we observe (see Fig. 1). It is clear from the geometry and from the behavior of the diffusion coefficient (see Fig. 2), that the passage of particles through the walls is quite severely restricted when  $K^* \approx 100$  and levels off at a low value, about 15% of the free-liquid value, for  $K^* \geq 1000$ , as indicated by the behavior of  $D_{\perp}$ .  $D_{\parallel}$ , however, is almost unaffected by the permeability of the walls to particles.

In the case of thermal conductivity both  $\lambda_{\parallel}$  and  $\lambda_{\perp}$  are reduced with decreasing permeability of the walls (see Fig. 1).  $\lambda_{\parallel}$  is less affected than  $\lambda_{\perp}$ , as might be expected and falls to about 75% for  $K^* \geq 500$  whereas  $\lambda_{\perp}$  falls to about 20% of the unconstrained-liquid value for

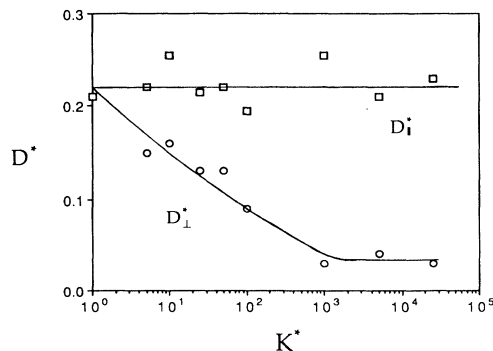


FIG. 2. For comparison, the components of the diffusion coefficient tensor  $D_{\perp}$  and  $D_{\parallel}$  for the same system as in Figs. 1 and 3.  $D^* \equiv (m/\varepsilon\sigma^2)^{1/2}D$ .

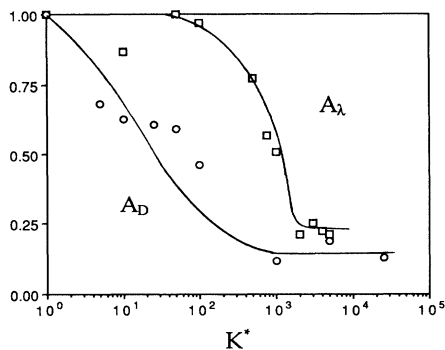


FIG. 3. As for Fig. 1, but plotted versus  $K$  on a logarithmic scale and for the anisotropy of the thermal conductivity,  $A_\lambda \equiv \lambda_\perp/\lambda_\parallel$ . For comparison the anisotropy of the diffusion coefficient  $A_D \equiv D_\perp/D_\parallel$  is also shown.

$K^* \geq 2000$ .

The corresponding anisotropy of the thermal conductivity,  $A_\lambda \equiv \lambda_\perp/\lambda_\parallel$ , as a function of  $K$ , on a logarithmic scale, is shown in Fig. 3. For comparison, we also show the anisotropy of the diffusion constant  $A_D \equiv D_\perp/D_\parallel$ .  $A_D$  falls more or less steadily as  $K$  increases (logarithmically), whereas  $A_\lambda$  tends to remain near unity until  $K^* \approx 100$ , i.e.,  $\lambda_\perp$  and  $\lambda_\parallel$  fall together at first. But then

the anisotropy sets in relatively abruptly. However, the limiting anisotropy is smaller than for diffusion. This behavior is as might be expected because restriction of the flow of atoms through the walls of the pore directly reduces the diffusion coefficient. The effect of changes of the permeability of the walls to particles is less effective in reducing the flow of energy because the flow is only in part translational, i.e., carried by the particles themselves. The translational part [first term in Eq. (5)] is, in fact, roughly one quarter of the total thermal conductivity only. The other potential part is carried through space by the interactions between the particles in the liquid and between the liquid particles and the wall particles. It is not particularly simple to explain the thermal conductivity of a homogeneous liquid [10]. We shall not attempt a quantitative explanation of the effective anisotropic thermal conductivity of this perturbed, constrained liquid in this preliminary report.

#### ACKNOWLEDGMENTS

This research was supported by a grant from the Chemical Sciences Division, U.S. Department of Energy (Grant No. DE-FG02-87ER13769). Travel funds were provided by NSF (INT-9123242) and NATO (CRG-910040). Computing services were provided by the University of Illinois Computer Center. J.G.P. acknowledges support from the Leverhulme Emeritus Foundation.

- [1] J. G. Powles, S. Murad, and P. Ravi, *Chem. Phys. Lett.* **21**, 188 (1992).
- [2] S. Murad, P. Ravi, and J. G. Powles, *J. Chem. Phys.* **98**, 9771 (1993).
- [3] D. J. Evans, *Phys. Lett.* **91A**, 457 (1982).
- [4] M. J. Gillan and M. Dixon, *J. Phys. C* **16**, 869 (1983).
- [5] D. J. Evans and G. P. Morris, *Statistical Mechanics of Nonequilibrium Liquids* (Academic, London, 1990).
- [6] J. G. Powles and M. Pogoda, *Molec. Phys.* **78**, 757 (1993).

- [7] *J. Chem. Soc. Farad. Trans.* **87**, 13 (1991).
- [8] J. Caro, M. Bulow, W. Schirmer, J. Karger, W. Heink, H. Pfeifer, and S. P. Zhdanov, *J. Chem. Soc. Faraday Trans. I* **81**, 2541 (1985).
- [9] C. Hoheisel and R. Vogelsang, *Comp. Phys. Rep.* **8**, 1 (1988).
- [10] J. P. Hansen and I. R. McDonald, *Theory of Simple Liquids* (Academic, London, 1986), Chap. 8.